Available online at www.sciencedirect.com

SCIENCE DIRECT®

Polymer 45 (2004) 2051–2060

polymer

www.elsevier.com/locate/polymer

Quantitative structure–property relationships for composites: prediction of glass transition temperatures for epoxy resins

Heping Liu[a,1], Alfred Uhlherr[a,*], Michael K. Bannister[b]

[a]CSIRO Molecular Science, Bag 10, Clayton South, Vic. 3169, Australia
[b]Cooperative Research Centre for Advanced Composite Structures Ltd, 506 Lorimer St, Fishermans Bend, Vic. 3207, Australia

Received 26 September 2003; received in revised form 9 January 2004; accepted 9 January 2004

Abstract

The glass transition temperatures of nine stoichiometric resin systems of tetraglycidyl-4,4′-diamino-diphenylmethane (TGDDM), triglycidyl *p*-amino phenol and diglycidyl ether of bisphenol A with 4,4′-diaminodiphenylsulphone (DDS), diethyl-toluenediamine and dimethylthiotoluenediamine were calculated using group interaction modelling (GIM) and atomic additivity (AA) methods. The input parameters were generated from kinetics simulation, which outputs the structure information for the cured systems. The modelling parameters were also applied to four non-stoichiometric systems of TGDDM and DDS. The predicted values from GIM were in good quantitative agreement with measured results from temperature modulated differential scanning calorimetry for all systems studied. Compared to GIM, the AA method gave inferior predictions for the highly crosslinked systems, especially for those, where epoxy was in excess.

Keywords: Quantitative structure–property relationships; Glass transition temperature; Epoxy resin

1. Introduction

The development of new materials involves extensive experimental work on trials under different conditions. Synthesis of polymers with desired properties is a challenging task which often involves considerable time and resources. The ability to predict the end product properties of the new materials is of great value because it provides a guide for the development process and speeds up the development cycle.

The most familiar and important property of polymeric and composite materials is the glass transition temperature, T_g. T_g determines the temperature windows for processing and utilizing these materials and is a prerequisite for the prediction and understanding of the mechanical and other properties.

There have been many methods proposed for predicting glass transition temperature in polymer systems. These include empirical equations [1–3], molecular dynamics simulation [4–7], semi-empirical methods [8] and mathematical tools including neural networks [9–11], fuzzy set theory [12] and graph theoretical indices [13,14]. Most of the empirical equations correlate the T_g with extent of conversion rather than the monomer structures; thus they cannot provide insight into the design of new materials. The mathematical fitting tools require large data sets which are not always available or are not consistent due to differences in measuring conditions. Although a detailed atomistic simulation approach to predicting polymer properties is very attractive in the long term, these simulations require expensive computational time to obtain practically useful results, and are still poorly suited to thermoset systems.

Many semi-empirical methods for devising quantitative structure–property relationships (QSPR) can perform reliable predictions for linear homopolymers. The most widely accepted and practically used QSPR approaches include: (1) Van Krevelen's group contribution method [15]; (2) Porter's group interaction modelling (GIM) [16]; (3) Bicerano's connectivity index method [13]; (4) Askadskii's atomic additivity (AA) method [17]. Seitz [18] also developed a set of correlations using group contributions for the prediction of polymer properties. Among these,

---

[*] Corresponding author. Tel.: +61-3-9545-8107; fax: +61-3-9545-2446. *E-mail address:* alfred.uhlherr@csiro.au (A. Uhlherr).

[1] Present address: Centre for Magnetic Resonance, The University of Queensland, St Lucia, QLD 4072, Australia.

0032-3861/$ - see front matter © 2004 Elsevier Ltd. All rights reserved.
doi:10.1016/j.polymer.2004.01.008

however, only GIM and AA are also intended to be applicable to crosslinked polymers.

It is the purpose of this study to develop a suitable protocol for predicting the glass transition temperatures of epoxy-based thermoset materials as a function of composition and processing conditions. We test this by evaluating the glass transition temperatures of some commonly used epoxy–diamine systems based on the structure information derived from kinetic simulation, and validate the predictions with experimental results.

2. Experimental

2.1. Materials

MY721 and MY720, which are, respectively, approximately 92 and 82% epoxy group equivalence of tetraglycidyl-4,4′-diamino-diphenylmethane (TGDDM), 4,4′-diaminodiphenylsulphone (DDS) and triglycidyl *p*-amino phenol (TGAP), were obtained from Vantico. Diglycidyl ether of bisphenol A (DGEBA) from the Dow Chemical Company was used. Ethacure® 100 or diethyltoluenediamine (DETDA), which exists as a mixture of 2,4 and 2,6 isomers, and Ethacure® 300 or dimethylthiotoluenediamine (DMTDA), which is a mixture of 2,4 and 2,6 isomers, were purchased from Albemarle® Corporation.

2.2. Sample preparation and characterisation

Stoichiometric ratios of epoxy and amine were mixed and cured at different temperatures, as shown in Table 1, for 3 h and then post-cured at 205 °C for 2 h in DSC pans. The experimental glass temperatures were obtained using alternating differential scanning calorimetry (ADSC) on a Mettler Toledo 821e equipped with an intracooler. STAR^e software was used for ADSC evaluation. An underlying heating rate of 1 °C/min, an amplitude of 1 °C and a period of 60 s were used to perform the ADSC scans.

The above systems were also cured in $120 \times 120 \times 3\ \mathrm{mm}^3$ moulds following the same temperature protocols. The cured samples were cut into $40 \times 10\ \mathrm{mm}^2$ strips and DMTA experiments were performed from 50 to 300 °C at 2 °C/min at a frequency of 1 Hz using three point bending geometry. The T_g was taken as the temperature corresponding to the peak of tan δ or as the extrapolated onset of the storage modulus.

Table 1
Curing conditions of different epoxy–amine systems

System	Cure temperature (°C)
TGDDM–DDS	160
TGDDM–DETDA	120
TGDDM–DMTDA	170
TGAP–DDS	140
TGAP–DETDA	130
TGAP–DMTDA	160
DGEBA–DDS	140
DGEBA–DETDA	100
DGEBA–DMTDA	150

Different stoichiometric ratios of MY720 and DDS were also prepared and cured at 160 °C for 3 h and then post-cured at 205 °C for 2 h in DSC pans. ADSC scans were performed at the same conditions as the stoichiometric systems.

3. Modelling method

3.1. Group interaction modelling

GIM uses the intermolecular energy of interaction between groups of atoms in adjacent polymer chains as a basis for predicting some important engineering properties of bulk polymers as a function of chemical composition and molecular structure [16]. The overall energy of molecular interactions can be expressed in the following equation:

$$\phi = -\phi_0 + H_C + H_T + H_m \tag{1}$$

where ϕ, ϕ_0, H_C, H_T and H_m are the overall energy of interaction, potential energy well, energy of configuration, thermal energy and mechanical energy, respectively. By applying some boundary conditions, relating the energy terms to model parameters and using generic values for a glassy polymer, glass transition temperature (T_g) can be expressed in the following form:

$$T_g = 0.224\theta + 51.3\frac{E_{coh}}{N} \tag{2}$$

where θ, E_{coh} and N are the reference temperature, cohesive energy and the number of degrees of freedom of a repeat unit. The reference temperature is related to the characteristic vibrational frequency of cooperative motion in the polymer chain axis. For polymers containing phenyl rings in the chain backbone, a single empirical value of 550 K can be used within experimental error [16]. Cohesive energy is the increase in internal energy per mole of material if all intermolecular forces are eliminated. Number of degrees of freedom is often used interchangeably with number of skeletal modes of vibration. Their values can be obtained through numerical group contributions [16].

For a linear polymer, it is easy to define the repeat unit if the monomer compositions are known. Thus, the cohesive energy and the number of degrees of freedom can be easily calculated via a range of means. However, for a crosslinked system, it is difficult to define the repeat unit because of the variation in crosslink density at different spots.

A crosslinked system can be arbitrarily broken into small fragments of epoxy and amine moieties. Some moieties may have the same basic chemical structure but different connections. For example, the moiety of a DGEBA molecule may be an unreacted monomer, or a linear chain unit, where two epoxides were reacted, or it may contain one crosslink point, where two epoxides and one hydroxyl were reacted, or have two crosslink points, where two epoxides and two hydroxyls were reacted. The same is true for the other molecules, where the maximum number of connections of a moiety equals the maximum number of functional groups. The individual cohesive energy and degree of freedom can generally be identified for each moiety. If the composition of these moieties in a system is known, then the average cohesive energy and degree of freedom values can be calculated. The modified glass transition temperature expression for our systems becomes:

$$T_g = 0.224\theta + 51.3\frac{E_{\mathrm{coh}}}{N} = 123 + 51.3\frac{\sum x_i E_{\mathrm{coh},i}}{\sum x_i N_i} \qquad (3)$$

where x_i, $E_{\mathrm{coh},i}$ and N_i are the composition, cohesive energy and rotational degree of freedom of the ith moiety.

The physical basis of the GIM method has been the subject of some recent debate, for example regarding the expressions for calculating storage and loss moduli [19]. For example the definition of Eq. (1) as a ‘balance between competitive intermolecular force components’ at the repeat unit level [16] differs somewhat from the standard laws of statistical mechanics. Nonetheless the formalism incorporates important monomer characteristics that govern material behaviour, such as cohesion and connectivity, in a manner that has proved intractable for alternative QSPR schemes. Hence GIM remains a potentially useful framework for empirical property correlations.

3.2. Atomic additivity

The AA method [17] is based on the representation of the repeating unit of the polymer in the form of a set of anharmonic oscillators which describe the thermal motion of atoms in the field of intra- and intermolecular forces, including weak dispersion forces, dipole–dipole interactions, hydrogen and valency bonds. The derived equation for glass transition temperature of a crosslinked system is:

$$T_g = \frac{\sum_i \Delta V_i}{\left(\sum_i a_i \Delta V_i + \sum_i b_i\right)_1 + \left(\sum_i K_i \Delta V_i\right)_p} \qquad (4)$$

where $\left(\sum_i a_i \Delta V_i + \sum_i b_i\right)_1$ is the set of increments for the linear fragments and $\left(\sum_i K_i \Delta V_i\right)_p$ is the set of increments for the crosslinked points, a_i is the constant related to the dispersion interaction of the ith atom with the adjacent atom of the repeating unit of the polymer, b_i is the constant characterising the contribution of each type of intermolecular interaction, K_i is the constant characterising the contribution of a crosslinked point to T_g and ΔV_i is the Van der Waals volume of atom i.

The same argument is applied to our system. Due to the difficulty in defining the repeat unit of the network, each fragment of the system is considered and the summation of the whole system is used to calculate T_g, and the above equation becomes:

$$T_g = \frac{\sum_j x_j\left(\sum_i \Delta V_i\right)}{\left(\sum_j x_j\left(\sum_i a_i \Delta V_i\right) + \sum_j x_j \sum_i b_i\right)_1 + \left(\sum_j x_j\left(\sum_i K_i \Delta V_i\right)\right)_p} \qquad (5)$$

where x_j is the composition of jth fragment. In this equation the parameter ΔV_i can be obtained from Ref. [17] which lists the values for each atom under different chemical environment. K_i, a_i and b_i are given in the same reference.

4. Results and discussion

4.1. Structural analysis

As is discussed in Section 3, due to the difficulty in defining a repeat unit of the crosslinked network, the monomer fragments with different reacted sites are to be used as the input structure parameters. The detailed analysis of these fragments is discussed in the following sections.

4.1.1. Amines

All the amines, DDS, DETDA and DMTDA, have two

Table 2
Possible DDS moieties formed during cure

n	Structure	E_{coh} (kJ/mol)	N'	N
0	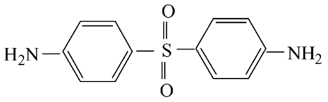	140.0	31	31
1	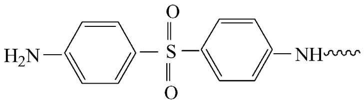	136.5	22	22
2	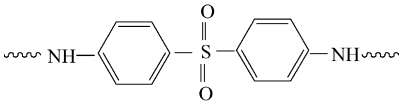	133.0	13	13
	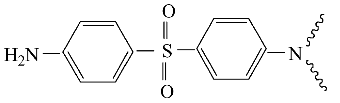	126.5	9	9
3	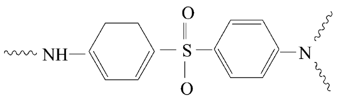	123.0	10	7
4	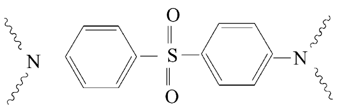	113.0	7	1

Table 3
Different TGDDM moieties formed during cure

n	Structure	E_{coh} (kJ/mol)	N'	N
0	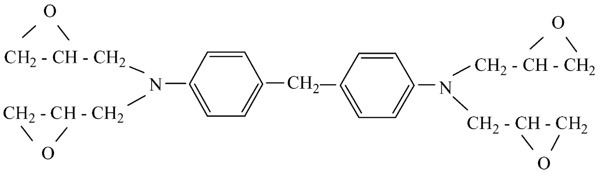	151.7	52	52
1	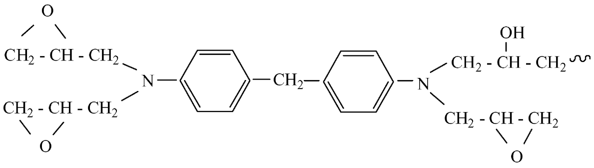	158.4	43	43
2	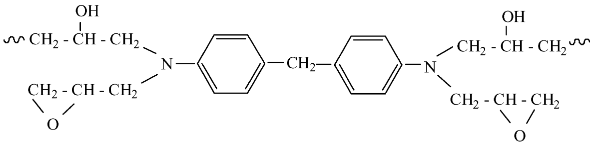	165.1	34	34
3	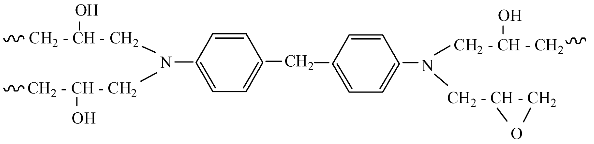	171.8	36	33
4	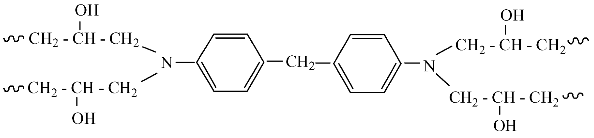	178.5	38	32
5	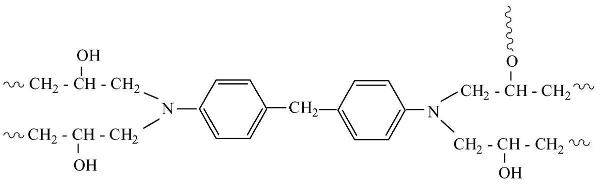	171.8	35	29
6	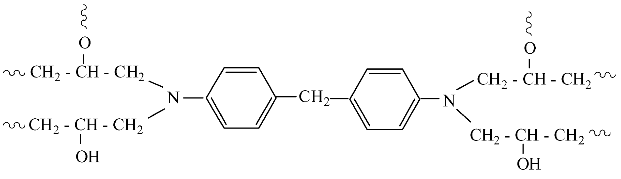	165.1	32	26
7	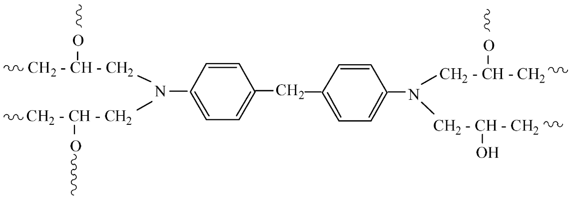	158.4	29	23
8	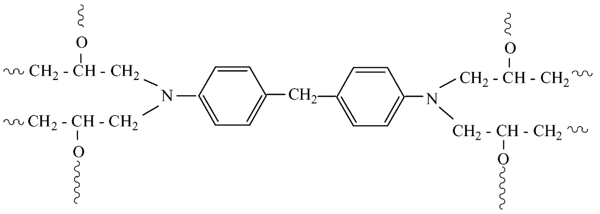	151.7	26	20

Table 4
Different major TGAP moieties formed during cure

n	Structure	E_{coh} (kJ/mol)	*N*
0	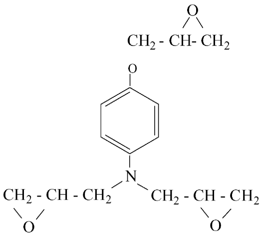	99.7	47
1	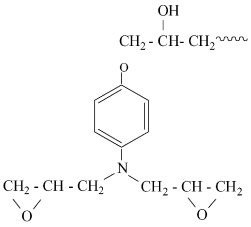 or 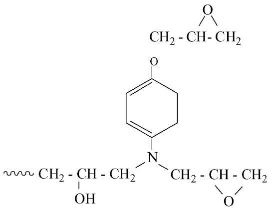	106.4	38
2	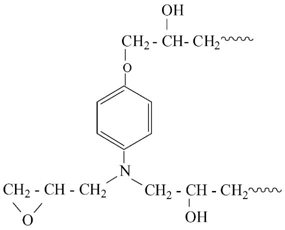	113.1	29
3	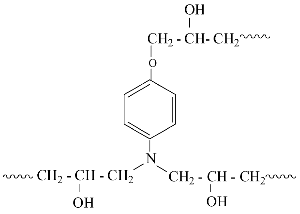	119.8	23
4	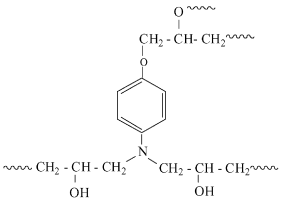 or 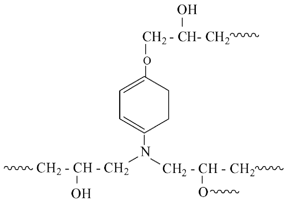	113.1	17
5	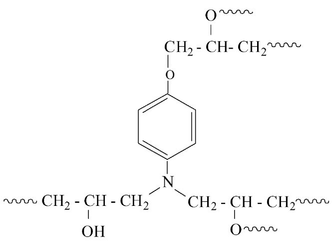	106.4	14
6	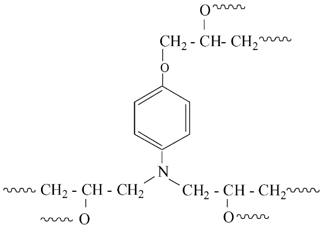	99.7	11

primary amine groups and thus are able to produce two secondary amine groups. The total functionality is four. If n is used to represent the number of reacted sites in an amine moiety, the possible products and their structures are listed in Table 2 using DDS as an example. When $n = 2$, although there are two possible structures, the first one predominates because the reactivity of the primary amine is higher than the secondary amine in DDS. The E_{coh} and N values are calculated using the empirical group contribution table [16].

4.1.2. TGDDM

TGDDM has four epoxide groups and can produce four hydroxyl groups when reacted. The total number of functionality is eight. The different major structures formed during cure are listed in Table 3. The other possible structures which are not the dominant species are not listed here; their influence on the calculation of T_g was evaluated and found to be negligible. Cohesive energies and degrees of freedom for each species were calculated accordingly using the group contribution table.

4.1.3. TGAP

TGAP has three epoxide functional groups and can produce three hydroxyl groups when reacted. The total number of functional groups is six. The major species are listed in Table 4, together with E_{coh} and N values. The other minor species have negligible effect on the T_g calculation.

4.1.4. DGEBA

DGEBA has two epoxide functional groups and can produce two hydroxyl groups when reacted. The total number of functional groups is four. The major species are listed in Table 5, together with E_{coh} and N values. The other minor species have negligible effect on the T_g calculation.

4.1.5. Hydroxy derivatives

The main impurities in epoxy–amine systems are those with hydroxyl groups [20]. To simplify the problem, the hydroxyl compounds are represented by the epoxy monomer with an epoxide group replaced by a hydroxyl group. The maximum numbers of functional groups in these derivatives are listed in Table 6. The same analysis is applied to these materials and the values of E_{coh} and N can be calculated.

4.2. Kinetic simulation

To find the compositions of different moieties in a reacted system, kinetic simulation is required to follow the cure process. Monte Carlo simulation, or random network simulation, has been widely applied in kinetics studies [21]. The commercial software DryAdd Pro from Oxford Materials Ltd is a generalised Monte Carlo package which simulates polymer chain growth and network formation in a 'reaction pot' and is especially applicable for crosslinked systems such as epoxy resins. The important input parameters are the components and their functional groups, the reactions between the functional groups and the absolute or relative reaction rates for each reaction. There are three principle reactions involved in the cure of epoxy–amine systems: (1) epoxide group reacts with primary amine to produce second amine; (2) epoxide group reacts with second

Table 5
Different major DGEBA moieties formed during cure

n	Structure	E_{coh} (kJ/mol)	N
0	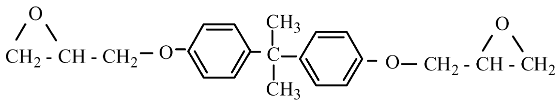	115.7	44
1	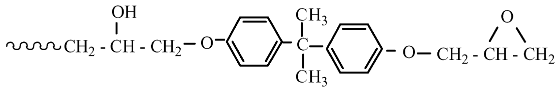	122.4	35
2	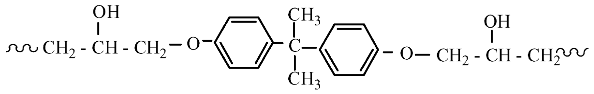	129.1	26
3	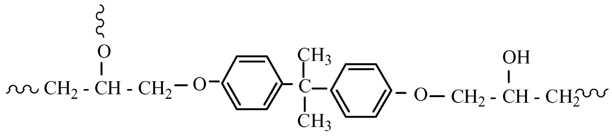	122.4	20
4	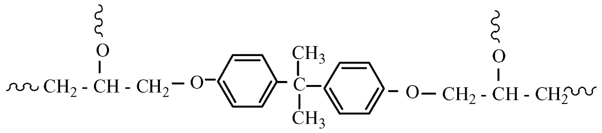	115.7	14

Table 6
Impurities in different systems and their functionalities

Epoxy	Structure	Max *n*
TGDDM–deri	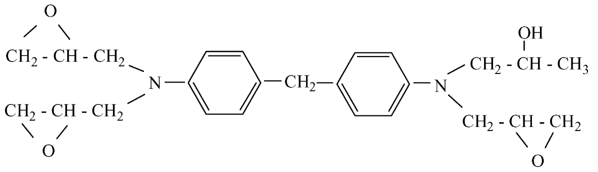	7
TGAP–deri	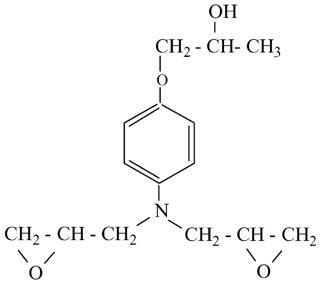	5
DGEBA–deri	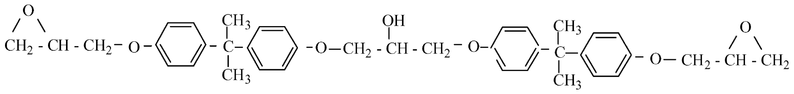	5

amine to produce tertiary amine; (3) epoxide group reacts with hydroxy to form an ether linkage. The reaction rate data are obtained from our study [22] or may in principle be calculated using quantum chemical methods. The important output from the kinetics simulation is the composition analysis of the network by number of reacted sites, which will be used in the T_g calculation.

Table 7 is a typical example of the results. It gives the number of molecules of different moieties having different reacted sites in the reaction pot. Knowing the total number of molecules, the percentage of each moiety can be obtained.

It can be seen from this result that, for DGEBA and its hydroxy derivative DGEBA-deri, the moieties with two epoxide groups and or with another hydroxyl group reacted are the main components. For DDS, the main component is the one with three functional groups reacted—two primary amine groups and one secondary amine group. The same analysis was performed for other systems and the main components for the different systems are listed in Table 8. The main components for epoxies are those with all epoxide groups reacted and those with one additional hydroxyl reacted. For amines the main components are those with two primary amines and one secondary amine reacted and those

Table 7
The compositions (in percentage to the whole system) of DGEBA/DDS system by number of reacted sites

Reacted sites (*n*)	DGEBA	DGEBA–deri	DDS
0	0.05	0.02	0
1	1.1	0.2	0.2
2	36.3	2.9	7.2
3	20.0	2.7	16.7
4	2.5	0.8	9.3
5		0.07	

Table 8
Number of reacted functional groups in the major components in different systems

System	Epoxy		Amine	
	n	Percentage[a]	*n*	Percentage[a]
TGDDM–DDS	4	38	3	45
	5	39	4	32
TGDDM–DETDA	4	56	3	27
	5	34	4	58
TGDDM–DMTDA	4	56	3	24
	5	33	4	60
TGAP–DDS	3	47	3	47
	4	38	4	29
TGAP–DETDA	3	59	3	38
	4	32	4	47
TGAP–DMTDA	3	65	3	25
	4	28	4	60
DGEBA–DDS	2	61	3	50
	3	33	4	29
DGEBA–DETDA	2	63	3	49
	3	31	4	29
DGEBA–DMTDA	2	71	3	41
	3	24	4	45

[a] Percentage to epoxy or amine only rather than the whole system.

with two primary amines and two secondary amines reacted. With the increasing relative reactivity of secondary amine from DDS, DETDA to DMTDA, the proportion of $n = 4$, where both secondary amines were reacted, increased.

4.3. Experimental T_g

The glass transition temperatures are measured by ADSC which is temperature modulated differential scanning calorimetry. It is based on the addition of a periodically varying temperature modulation to the linear heating (or cooling) rate, which has been applied extensively in the study of the glass transitions [23–25]. The epoxy systems studied in this work are all post-cured and have high T_g values. With the conventional DSC, the glass transition of the highly crosslinked TGDDM and TGAP systems are very difficult to identify (Fig. 1). However, with ADSC, they are easily seen in either the reversing heat flow curves, the complex heat capacity curves, the in-phase heat capacity curves or the out-phase heat capacity curves, as is shown in Fig. 2 for the fully cured TGDDM/DETDA systems. For convenience, the glass transition temperatures were taken from the reversing heat flow curves, by measuring the midpoints of the abrupt change. These T_g values are listed in Table 9.

T_g values were also obtained from DMTA measurements, both the peak of tan δ and the onset of the storage modulus, and are listed in Table 9.

4.4. GIM prediction

Looking at the modelling parameters in Tables 2 and 3, it is notable that, for the different fragments from the same monomer, the change in cohesive energy is not very significant, but the change in N is dramatic. According to the GIM rules, if four or more chains converge to a single site, a full constraint in three dimensions exists, and six degrees of freedom are lost at each chain end [16]; for three chains converging on a single site, three degrees of freedom are lost per chain termination site. A set of degrees of freedom were calculated based on these rules and are listed in Tables 2 and 3 as N'. Using these parameters, the calculated T_g for the stoichiometric TGDDM/DDS system is 182 °C, which is much lower than the experimental value of 267 °C. Other systems were also tried with the same rules and the calculated values are all much lower than the experimental results. Alternative approaches for calculating the cohesive energy, such as the Bicerano method, were also tried. However, these give only small numerical variations, which are dwarfed by the sensitivity of T_g to the network connectivity as specified by the degrees of freedom.

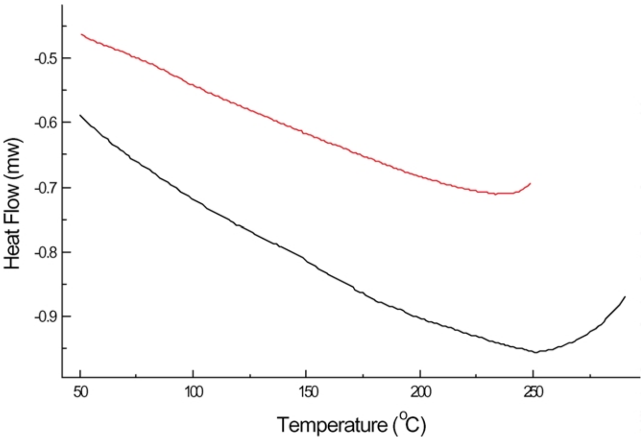

Fig. 1. DSC curves of post-cured TGDDM/DETDA (top) and TGAP/-DETDA (bottom) systems with a heating rate of 10 °C/min.

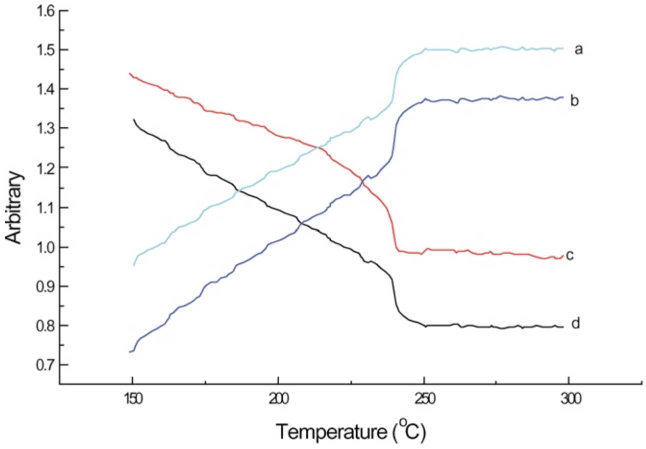

Fig. 2. ADSC curves of post-cured TGDDM/DETDA systems: (a) complex heat capacity; (b) in-phase heat capacity; (c) out-phase heat capacity; (d) reversing heat flow.

These findings indicate that N needs to be re-evaluated. Here we simply define 6 degrees of freedom lost for every additional branch point [8]. Note that this reduction is partially offset when the branch formation causes an epoxy sidegroup to become part of the polymer backbone, with an attendant increase in the number of backbone modes. Using the new sets of degrees of freedom listed in Tables 2 and 3 (column N), the calculated T_g is 265 °C, which is much closer to the experimental data. These sets of parameters for TGDDM were tested in TGDDM/DETDA and TGDDM/DMTDA stoichiometric systems, and the parameters for

Table 9
Experimental and predicted T_g values of different epoxy–amine systems

System	T_g (ADSC) (°C)	T_g (GIM) (°C)	T_g (DMTA) (tan δ, °C)	T_g (DMTA) (onset, °C)
TGDDM–DDS	267	262	281	269
TGDDM–DETDA	241	231	255	242
TGDDM–DMTDA	232	226	249	239
TGAP–DDS	266	275	281	266
TGAP–DETDA	245	240	265	250
TGAP–DMTDA	239	229	234	202
DGEBA–DDS	205	201	219	200
DGEBA–DETDA	173	180	206	188
DGEBA–DMTDA	171	171	193	179

DDS were tested in the TGAP/DDS and DGEBA/DDS systems. The predicted T_g values are in good agreement with the experimental data. The same rules were applied to the other systems and the values for N and the predicted T_g are listed in Table 9, as well as the experimental T_g obtained by ADSC.

The calculated T_g values are generally lower than the experimental results but the differences are within 10 °C, which demonstrate the capability of this method. It should also be noted that the experimental T_g depends on the heating rate, modulation frequency and period of modulation [24], and thus a moderate discrepancy is to be expected. The experimental T_g values also depend on the technique used. To emphasize this point, T_g values from DMTA are compared with the ADSC data. It is well known that the ADSC T_g values are generally much lower than those from tan δ peaks, but very close to the onset of the storage modulus [26]. An amorphous polymer changes from a glass to a rubber-like phase at the glass transition temperature, which is a temperature range. The different techniques pick up a single temperature within this range. In the GIM model, the glass transition temperature is described as the temperature at which repeat units in an amorphous polymer can undergo large-scale translation motion relative to each other. Adjacent groups are held together by the intermolecular cohesive forces. Eq. (2) relates T_g to the cohesive energy and the intramolecular (vibrational) degrees of freedom in the quiescent state. Since DSC measures T_g through the change of heat capacity rather than through a deformation mechanism, it is not surprising that the GIM predicted T_g values are closer to the DSC values than the DMTA values.

Considering the different systems in this study, it is also noticed that the predicted T_g values for the DGEBA systems are closest to the experimental results. This might be explained by its low functionality. DGEBA, TGAP and TGDDM have two, three and four epoxide groups, respectively. It is expected that, for the stoichiometric ratio systems, TGDDM and TGAP gel at lower conversions than DGEBA [27]. Thus, the networks formed in TGDDM and TGAP are expected to be less homogeneous than DGEBA, with intramolecular reactions and local cyclization. These effects would have an impact on the degree of freedom of the moieties involved and will be investigated further.

In addition to comparing the absolute values, it is also important to compare the general trend in predicted and experimental data. For the systems with the same epoxy resin, predicted T_g values decrease from DDS, DETDA to DMTDA, which is in good agreement with the trend found from ADSC. The DDS structure has two benzene rings which confer high rigidity and large cohesive energies and thus give a high predicted T_g. The major moieties of DMTDA have fewer degrees of freedom than DETDA due to the difference in SCH_3 and CH_2CH_3. For the systems with the same amine, the predicted T_g values for TGAP are slightly higher than TGDDM and much higher than DGEBA. This is also in good agreement with the experimental results. Although TGDDM has more epoxide groups in each monomer and has higher cohesive energy than TGAP and DGEBA, its major moieties also have greater degrees of freedom. These two effects cancel each other to some extent such that TGAP systems give a slightly higher T_g. The cohesive energies for major DGEBA moieties are slightly higher than TGAP but they also have greater degrees of freedom. The effect from the degrees of freedom outweighs the cohesive energy, thus giving a lower T_g.

4.5. Non-stoichiometric systems

To further validate the prediction using the above modelling parameters, non-stoichiometric systems were studied. The experimental and predicted T_g values for four different systems of TGDDM (MY720) and DDS with stoichiometric ratios (amine/epoxide) of 0.6, 0.9, 1.2 and 1.6 are listed in Table 10. The predicted T_g values agree well with the experimental results, and the trend is the same in experimental and predicted values, with system $r = 0.9$ having the highest value. The prediction for system $r = 1.6$, where excess amine exists, is not as accurate but still satisfactory.

The accuracy in estimating the concentration of the TGDDM-hydroxyl component in MY720 also has an effect on the predicted T_g values. MY720 has a lower epoxide group density than MY721. In the kinetics simulation to generate structure composition parameters, the TGDDM-hydroxyl concentration was taken as 0.38 kg/mol as reported [28]. To demonstrate the influence of this input parameter on the predicted T_g values, an arbitrary concentration of 0.3 mol/kg was used to generate a new set of T_g values which are listed in Table 10 as T_{g2} (GIM). Comparing this new set of values with the previous predicted figures, it can be seen that the decrease in the TGDDM-hydroxy concentration results in an increase of predicted T_g. This is expected because less TGDDM-hydroxy implies more TGDDM, which has a higher functionality.

Table 10
Experimental and predicted T_g values for non-stoichiometric TGDDM/DDS systems

Stoichiometric ratio r	T_g (ADSC) (°C)	T_g (GIM) (°C)	T_{g2} (GIM) (°C)	T_g (AA) (°C)
0.6	260	255	257	322
0.9	265	259	265	289
1.2	257	255	256	263
1.6	248	238	239	238

Table 11
Modelling parameters using atomic additivity method for the major fragments of TGDDM and DDS (n, number of reacted sites)

Resin	n	$\sum \Delta V_i$	$\sum a_i \Delta V_i$	$\sum b_i$	$\sum K_i \Delta V_i$
TGDDM	3	416.2	1.66	−0.64	0.065
	4	421.6	1.62	−0.72	0.129
	5	414.7	0.269	−0.64	0.174
	6	407.8	1.01	−0.552	0.219
	7	400.9	0.706	−0.468	0.264
DDS	2	200.3	0.751	−0.441	0
	3	198.3	0.638	−0.357	−0.096
	4	196.3	0.524	−0.273	−0.192

4.6. Atomic additivity prediction

Alternative methods for predicting T_g were also tried with less satisfactory results. For example, the AA method was applied to the above non-stoichiometric systems. The composition data were generated using kinetic simulation and the parameters for major moieties are listed in Table 11. Using Eq. (5), T_g values for the four systems were calculated and listed in Table 10 as T_g (AA). Comparing these values with the ADSC results, the predictions for systems $r = 0.6$ and $r = 0.9$ are much higher than the experimental values. In addition, the observed trend is qualitatively different from the experimental findings, with T_g decreasing rapidly with increasing amount of amine.

However, these results do not diminish the capability of the AA method. This appears more suitable for predicting glass transition temperatures of crosslinked systems such as elastomers, where crosslink density is not very high. For highly crosslinked systems like epoxy resin, the modelling parameters may need to be readjusted and to be further investigated.

5. Conclusion

Kinetics simulation and GIM can be combined to predict the glass transition temperatures of epoxy–amine thermoset systems, by utilizing the structural output of the former as compositional input to the latter. Special attention needs to be paid to the optimum definition of the number of degrees of freedom for each repeat unit moiety. This approach gives good agreement with experimental ADSC results for a full range of epoxy resin systems formed from three different epoxies and three different diamines with different functionalities. Good agreement was also obtained for non-stoichiometric systems of TGDDM and DDS. The results show that the difference in epoxy or amine structure has a significant impact on the glass transition temperature. Comparison of GIM versus AA methods for the non-stoichiometric systems indicates that the former gives superior T_g predictions for these resins.

Acknowledgements

We would like to thank Dr John Chiefari, Dr Russell Varley and Dr Wendy Tian of CSIRO and Mr Paul Andrews and Dr Ruxandra Rosu from CRC-ACS for valuable discussions.

References

[1] Won YG, Galy J, Pascault JP. J Polym Sci Polym Phys 1991;29(8):981.
[2] Venditti RA, Gillham JK. J Appl Polym Sci 1997;64(1):3.
[3] DelRio C, MartinAlvarez PJ, Acosta JL. Polym Bull 1997;38(3):353.
[4] Tan TTM, Rode BM. Macromol Theor Simul 1996;5(3):467.
[5] Han J, Gee RH, Boyd RH. Macromolecules 1994;27(26):7781.
[6] Pozuelo J, Baselga J. Polymer 2002;43(22):6049.
[7] Tsige M, Taylor PL. Phys Rev E 2002;65(2). art no 021805 part 1.
[8] Gumen VR, Jones FR, Attwood D. Polymer 2001;42(13):5717.
[9] Ulmer CW, Smith DA, Sumpter BG, Noid DI. Comput Theor Polym Sci 1998;8(3–4):311.
[10] Mattioni BE, Jurs PC. J Chem Inform Comput Sci 2002;42(2):232.
[11] Joyce SJ, Osguthorpe DJ, Padgett JA, Price GJ. J Chem Soc Faraday Trans 1995;91(16):2491.
[12] Sun H, Tang YW, Zhang FS. J Polym Sci Polym Phys 2002;40(19):2164.
[13] Bicerano J. Prediction of polymer properties. New York: Marcel Dekker; 1996.
[14] Garcia-Domenech R, de Julian-Ortiz JV. J Phys Chem B 2002;106(6):1501.
[15] Van Krevelen DW. Properties of polymers, 3rd ed. Amsterdam: Elsevier; 1990.
[16] Porter D. Group interaction modelling of polymer properties. New York: Marcel Dekker; 1995.
[17] Askadskii AA. Physical properties of polymers: prediction and control. Amsterdam: Gordon and Breach; 1996.
[18] Seitz JT. J Appl Polym Sci 1993;49:1331–51.
[19] Davis WM, Szabo JP. Prediction of the dynamic mechanical properties of polymers II: group interaction modelling. Chem Prepr 2001; http://preprint.chemweb.com/physchem/0111005.
[20] St John NA, George GA. Prog Polym Sci 1994;19:755.
[21] Cheng KC, Don TM, Rwei SP, Li YC, Duann YF. J Polym Sci Polym Phys 2002;40(17):1857.
[22] Liu H, Uhlherr A, Varley RJ, Bannister MK. Submitted for publication.
[23] Jones KJ, Kinshott I, Reading M, Lacey AA, Nikolopoulos C, Pollock HM. Thermochim Acta 1997;304–305:187.
[24] Montserrat SJ. Therm Anal Calorim 2002;59(1–2):289.
[25] Gmelin E. Thermochim Acta 1997;304–305:1.
[26] Ramis X, Cadenato A, Morancho JM, Salla JM. Polymer 2003;44:2067.
[27] Stepto RFT, editor. Polymer networks—principles of their formation, structure and properties. London: Blackie Academic and Professional; 1998.
[28] St John NA, George GA, Cole-Clarke PA, Mackay ME, Halley PJ. High Perform Polym 1993;5:21.